Channel Parameter Studies with a Biocompatible Testbed for Molecular Communication: Methods and Data

Max Bartunik [1], Janina Teller [2], Georg Fischer [2], and Jens Kirchner [2]

[1]Friedrich-Alexander-Universität Erlangen-Nürnberg (FAU)
[2]Affiliation not available

October 30, 2023

Abstract

Testbeds play an essential role in the development of real-life molecular communication applications and experimental validation of communication channel models. Although some testbed concepts have been published in recent years, very few setups are inherently suitable for biomedical applications. Furthermore, systematic experimental data of a wide parameter field for molecular communication is scarce and often difficult to generate. In this work, a biocompatible testbed for molecular communication with magnetic nanoparticles is used to investigate a series of transmission channel parameters. The observed results are discussed in the context of a laminar flow channel. All experimental data regarding the parameter studies as well as an additional data set for a large binary transmission sequence is provided as a supplement to this publication. The data is available on a public server to allow for further use by other researchers.

Channel Parameter Studies with a Biocompatible Testbed for Molecular Communication: Methods and Data

Max Bartunik, Janina Teller, Georg Fischer, Jens Kirchner

***Abstract*—Testbeds play an essential role in the development of real-life molecular communication applications and experimental validation of communication channel models. Although some testbed concepts have been published in recent years, very few setups are inherently suitable for biomedical applications. Furthermore, systematic experimental data of a wide parameter field for molecular communication is scarce and often difficult to generate. In this work, a biocompatible testbed for molecular communication with magnetic nanoparticles is used to investigate a series of transmission channel parameters. The observed results are discussed in the context of a laminar flow channel. All experimental data regarding the parameter studies as well as an additional data set for a large binary transmission sequence is provided as a supplement to this publication. The data is available on a public server to allow for further use by other researchers.**

***Index Terms*—molecular communication, nanoparticles, spions, parametric data, methods, testbed**

I. Introduction

Molecular communication can be used to establish a communication link in environments where conventional electromagnetic communication is infeasible [1], such as in a medical scenario with a restricted power source. Instead of electromagnetic waves, information particles are used to propagate information in a gaseous or fluid channel (e.g. the cardiovascular system) [2]–[6]. In a medical scenario it is essential to use biocompatible information particles with little to no interaction with the biological environment.

Although the concept of engineered molecular communication was suggested two decades ago [7], experimental setups using molecular communication have only been presented in recent years, with only few setups that are principally suitable for medical applications amongst these publications.

Some of the first experimental work in molecular communication used alcohol to transmit information through air (i.e. a gaseous environment) as a medium [2]. This concept was extended and applied by various other works [8]–[14]. Similarly, air-based communication with other information particles, such as fluorescent particles [3] or odours [15], [16] has also been proposed. However, as systems using gaseous environments are typically not applicable to a medical context, we will focus on fluid-based testbeds.

Experimental setups for fluid environments using a wide range of information carriers, such as glucose [17], salt [18], [19], or pH value [5], [6], [20], [21], have been constructed. Applications to biomedical contexts were specifically regarded in [18], where a pharmacokinetic model as a method for data transmission in the human body was modelled, and [17], where glucose concentration was modulated in a biocompatible setup. In [22], data transmission using the concentration of DNA strands was investigated. However, the experiment involved an offline manual sampling procedure and cannot be used for continuous transmissions.

Principally, the use of materials which are naturally present in the used biological environment (such as glucose or salt) as information carriers, will be very restricted and subject to significant environmental interference (e. g. homeostasis). Many medical applications, such as communication in a blood vessel, will therefore not be feasible. In contrast, the concept presented in [4], on which this paper is based, relies on artificially synthesised magnetic nanoparticles (specifically superparamagnetic iron-oxide nanoparticles, or SPIONs) to encode information. The used SPIONs have been shown to be biocompatible [23], [24] and are therefore suitable for medical applications.

The work presented here is based on a testbed using SPIONs in a background flow of water, published in [25]. In previous work, SPIONs were detected at the receiver using either inductive setups with wire-wound coils [26]–[28] or a capacitance sensor [29]. Here, we will be using planar coils with an inductive sensor [30]. In contrast to wire-wound coils, these are easier to manufacture and can be placed on the outside of a transmission channel instead of requiring the channel to be passed through the sensor coil. They are therefore an essential improvement for an application scenario.

Acquisition of real testbed data is an essential factor to understanding processes in molecular communication and verifying system models. This paper therefore provides a set of experimental data, investigating a variety of transmission channel parameters. Furthermore, large sets of data, containing two transmission samples with 1000 pulses with different symbol intervals are provided.

II. Testbed

The experimental setup can principally be split into the components transmitter, channel, and receiver. The transmitter injects SPIONs into the transmission channel to modulate the concentration of nanoparticles observed at the receiver over time. The channel is typically set by the application scenario and has an active background flow.

M. Bartunik, J. Teller, G. Fischer and J. Kirchner are at the Institute for Electronics Engineering, Friedrich-Alexander-University Erlangen-Nürnberg (FAU).

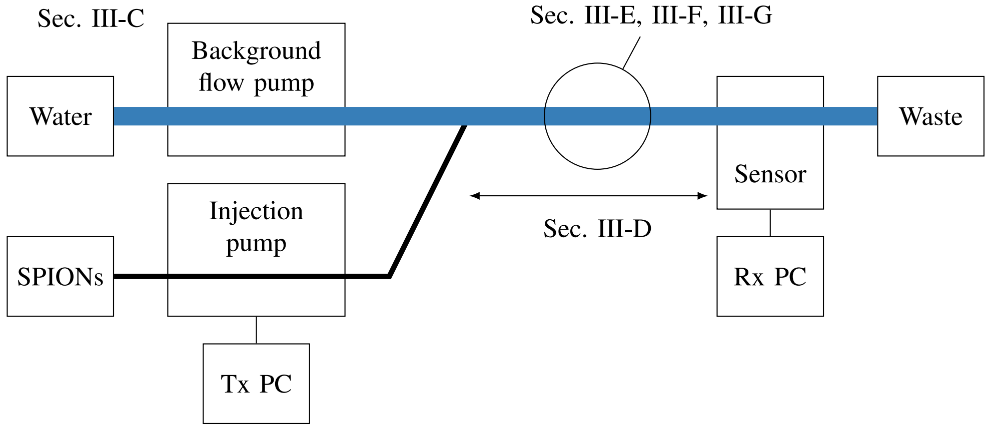

Fig. 1: Components of the investigated testbed setup. A pump is used to inject SPIONs into a channel with a constant background flow of water. They are detected at the receiver using an inductive sensor with planar coils. The components that were modified in parameter studies (background flow rate, channel length, channel diameter, channel geometry) are annotated with the appropriate section references.

An overview of the testbed setup, annotated with the parameter variations investigated in Sec. III, is provided in Fig. 1.

A. Transmitter

Either a peristaltic pump (Ismatec Reglo ICC[1]) or micropump (Bartels mp6-liq[2]) is used to inject SPIONs into the background flow in this work. The peristaltic pump has a high forward flow pressure, enabling consistent dispensing with changing output pressures. It is used for the experiments regarding different transmission channel parameters. Due to its compact size, the micropump is more applicable to real-life setups. It was therefore used for the modulated injections in the data transmission samples.

The peristaltic pump was controlled from a PC via a USB-connection using the software tool provided by the manufacturer (Ismatec Pump Control). The micropump was operated using the manufacturers driver and interface (Bartels mp-Highdriver4[3] and mp-Multiboard[3]), controlled from a Python script.

The pump was connected to the transmission channel using flexible tubing (Tygon LMT-55, 1.52 mm inner diameter) and a venous cannula with a diameter of 0.7 mm. The cannula was inserted into the transmission channel, along the direction of flow, to then remove the needle.

B. Information Carriers

The SPIONs used as information particles, were manufactured by the Section for Experimental Oncology and Nanomedicine of the University Hospital in Erlangen [23]. They consist of an iron core and a biocompatible coating of lauric acid to avoid agglomeration. They typically have a hydrodynamic radius of 50 nm and were used at a stock iron concentration of 7.5 mg/mL, suspended in water. The nanoparticles are biocompatible and have been used in other medical applications, such as drug targeting [31].

The magnetic properties of the SPIONs (i.e. a high susceptibility and no remanence) can be used to detect the nanoparticles using susceptometers or other devices capable of detecting the change of an electromagnetic field.

[1] us.vwr.com/store/product/39213403/masterflex-ismatec-reglo-independent-channel-control-icc-peristaltic-pumps-avantor

[2] www.bartels-mikrotechnik.de/en/micropumps/

[3] www.bartels-mikrotechnik.de/en/microelectronics/

TABLE I: Reynolds number for a selection of used channel parameters. In all cases $Re \ll 2300$ holds.

Volumetric flow rate	Tube diameter	Reynolds number
2 mL/min	1.52 mm	28
10 mL/min	1.02 mm	208
10 mL/min	1.52 mm	139
10 mL/min	2.79 mm	76
10 mL/min	3.17 mm	67
20 mL/min	1.02 mm	415
20 mL/min	1.52 mm	279

C. Channel

As for the particle injection, flexible tubing is used as the transmission channel. In most cases, a channel with an inner diameter of 1.52 mm and a constant water flow of 10 mL/min, upheld by the peristaltic pump, was used.

The Reynolds number Re can be used to determine the applicable flow regime for the used setup. For fluids, with the density ρ (998 kg/m^3 for water at normal temperature and pressure) and dynamic viscosity μ (1×10^{-3} kg/(m s)), in a smooth circular pipe with diameter d

$$Re = \frac{\rho V d}{\mu} < 2300 \tag{1}$$

must be fulfilled to ensure a laminar flow regime [32]. The velocity v can be calculated from the volumetric flow rate Q as

$$v = Q \frac{4}{\pi d^2}. \tag{2}$$

Due to the channel geometry, we can typically observe a laminar flow profile, with a high velocity in the centre and close to zero velocity at the edges, inside the tube. The laminar flow causes an injected particle burst to be distributed axially with a high initial concentration and a long (theoretically infinite) trailing response. Tab. I shows the Reynolds number for a selection of channel parameters used in this work. In all cases the criterion for laminar flow is met.

D. Receiver

The SPIONs are detected at the receiver using an inductive sensor with a planar coil [30]. As the nanoparticles pass by the planar coil, their susceptibility causes a shift of the coils inductance, which can in turn be detected as a change in resonance frequency of a parallel resonant circuit. This is achieved using the inductance to digital converter LDC1614[4] from Texas Instruments, paired with a coil (29 mm diameter, 30 turns per layer, 4 layers) selected from the LDCCOILEVM[5] kit and a 68 pF capacitor. The coil used here was chosen from a variety of different geometries as it showed a good sensitivity in the testbed setup [30].

The sensor was operated with the manufacturers software (Sensing Solutions EVM GUI from Texas Instruments[4]) at an effective sampling rate of approx. 50 Sa/s.

III. Parameter Variations

As we specifically want to investigate the behaviour of the molecular communication channel under different physiological conditions, a variety of channel parameters and geometries were evaluated regarding their impulse response.

A. General Measurement Procedure

In all cases, a train with ten bursts of SPIONs, separated by a delay of 30 s to allow for a return to the baseline concentration, was injected using the peristaltic pump. Each burst consisted of 30 µL of the stock suspension and was injected at a flow rate of 10 mL/min. Before each measurement, an initial pulse of SPIONs was injected to ensure an identical state of the injection pathway throughout experiments (initialisation). The sequence is illustrated in Fig. 2.

If not specified otherwise, the receiver (i.e. the starting edge of the sensor coil) was placed at a distance of 50 mm from the tip of the injection cannula, the background flow was set to a flow rate of 10 mL/min, and the transmission channel had an inner diameter of 1.52 mm.

B. Data Analysis

The recorded data was evaluated using MATLAB (MathWorks). First, the raw data samples were offset corrected to a zero baseline by subtracting the overall minimum and interpolated using linear interpolation to a consistent sample rate of 100 Sa/s, eliminating inaccuracies in the sampling intervals caused by inconsistent transmission delays. Then, a moving-average filter with a width of ten samples was applied to reduce environmental noise. The filtered data set was split

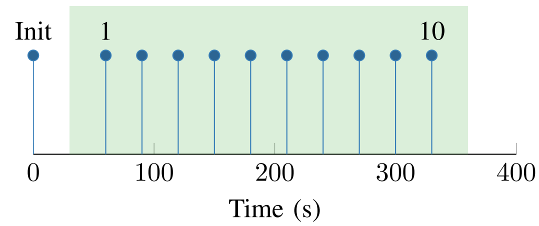

Fig. 2: Test procedure containing an initial burst (Init) and a train of ten injections (blue). Each injection burst has a duration of 0.18 s. The recorded measurement window is shown in green.

into individual segments, each containing the response to one injection burst, to then synchronise the segments by maximising the cross-correlation between the impulse responses. Finally, the responses were averaged, eliminating the two strongest outliers.

Two key performance indicators (KPIs) to characterise the impulse responses were evaluated, namely the maximum amplitude and full width at half maximum (FWHM). They are assessed for each data segment, to then determine an average with standard deviation of the complete data set.

C. Background Flow

A parameter with a substantial influence on the distortion of the injected pulse during transmission is the rate of the background flow in the transmission channel. In a real-life application this will typically be a pre-set condition, such as the flow rate of a specific blood vessel. In the testbed, the background flow, driven by a peristaltic pump, was varied over a decade from 2 to 20 mL/min (similar to e. g. the flow rate in a foot [33] or hand [34] artery).

As we can see in Fig. 4 (see Fig. 3 for average impulse responses), the maximal amplitude decreases as the flow rate of the background flow increases. This corresponds to a higher dilution ratio of the injected SPION bursts. As the flow rate changes, so does the velocity and therefore the observed duration of the nanoparticles at the receiver. Additionally, the initial distribution is changed with the relative flow rate of the injection. By normalising the FWHM t_{FWHM} to the ratio of injection flow rate Q_{inj} to background flow rate Q_{channel} and $t_{\mathrm{FWHM}} \mid Q_{\mathrm{inj}} = Q_{\mathrm{channel}}$ as reference, according to

$$t'_{\mathrm{FWHM}} = \frac{Q_{\mathrm{channel}}}{Q_{\mathrm{inj}}} \frac{t_{\mathrm{FWHM}}}{t_{\mathrm{FWHM}} \mid Q_{\mathrm{inj}} = Q_{\mathrm{channel}}}, \tag{3}$$

the change of FWHM caused by an increased observation duration with the change in velocity can be eliminated. The normalised FWHM (dimensionless) in Fig. 4 shows a slight increase for the highest flow rates, corresponding to a change in injection dynamic (e. g. more turbulence at the point of injection). Nonetheless, we can observe that a potentially different relative background flow rate only has a minor effect on the initial distribution of an injected burst of SPIONs.

D. Channel Length

The maximally usable channel length is an important factor when implementing a molecular communication system. As

[4]www.ti.com/product/LDC1614
[5]www.ti.com/tool/LDCCOILEVM

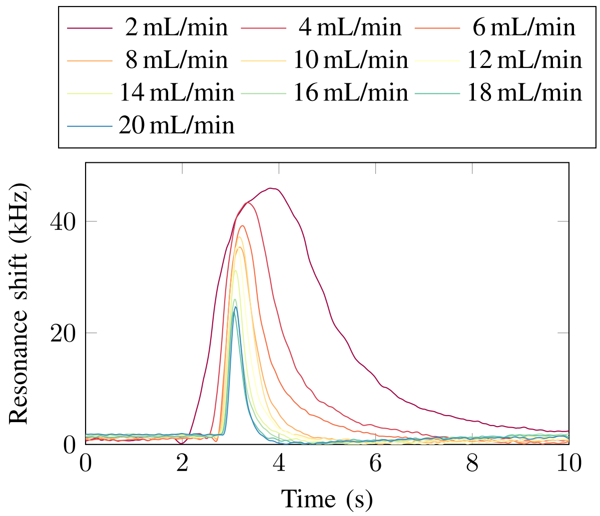

Fig. 3: Impulse responses for different background flow rates in the transmission channel ranging from 2 to 20 mL/min.

in electromagnetic transmissions, an increased channel length will have a negative impact on the quality of the received signal. Multiple short sections may be cascaded to establish long communication links.

In molecular communication the observed distances are typically very small, up to the centimeter range. The testbed response was evaluated for distances in the range of 50 mm to 350 mm using the same procedure as before.

As the channel length increases, the axial distribution of the injected SPION burst, due to laminar flow in the transmission channel, also widens and causes both a reduction of the peak amplitude and a larger half maximum duration. As can be seen in Fig. 5, this effect is very pronounced for channel lengths of 300 mm and above. At these lengths, the duration measurement has a large deviation due to the small amplitude. The relative increase of noise is also visible in the average impulse responses shown in Fig. 6.

E. Channel Diameter

Large variations of the channel diameter can have a significant influence on the transmission behaviour as different flow regimes become dominant. However, in the context of this testbed we will only observe parameters within the laminar flow domain. The aforementioned measurement procedure was repeated with the original tube with a diameter of 1.52 mm and three other tubes with the diameters 1.02 mm, 2.79 mm, and 3.17 mm.

Fig. 7 shows the observed FWHM at the receiver, which increases consistently with the transmission tube diameter. This behaviour corresponds to a reduction of the average velocity, as defined by Eq. 2. Large variations in amplitude and pulse shape (see Fig. 8) can be observed. However, due to the variety of potential influence factors (ratio of injection cannula diameter to channel diameter, average flow velocity, distribution behaviour at point of injection) these cannot be clearly attributed to a specific physical effect.

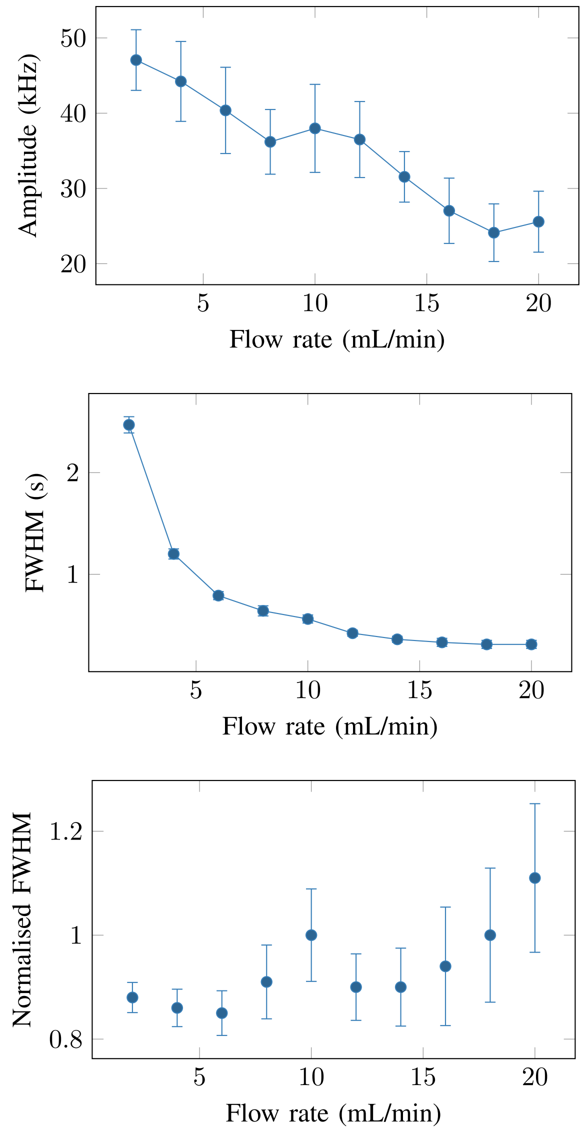

Fig. 4: Amplitude, FWHM, and FWHM normalised to the ratio between injection and background flow rate observed at the receiver for different background flow rates. An increase in background flow (and therefore velocity) causes a reduction of maximal amplitude as the injected burst gets diluted more and leads to a smaller FWHM duration.

F. Bent Channel

So far, we have observed an unobstructed and straight channel from the transmitter to the receiver. We will now investigate the changes in impulse response when the channel is bent at different angles in the middle between transmitter and receiver. To this end, a special rig with well-defined angles was manufactured with a 3D-printer. The transmission channel was then placed into the various angle positions (35° to 180°) and the impulse response evaluated as before. Due to the additional space required for the bending rig, the channel length was chosen as 100 mm.

The results in Fig. 9 show no consistent overall trend. However, a higher FWHM can be observed for the sharp angles ($\leq 90°$). This is caused by a collection of nanoparticles

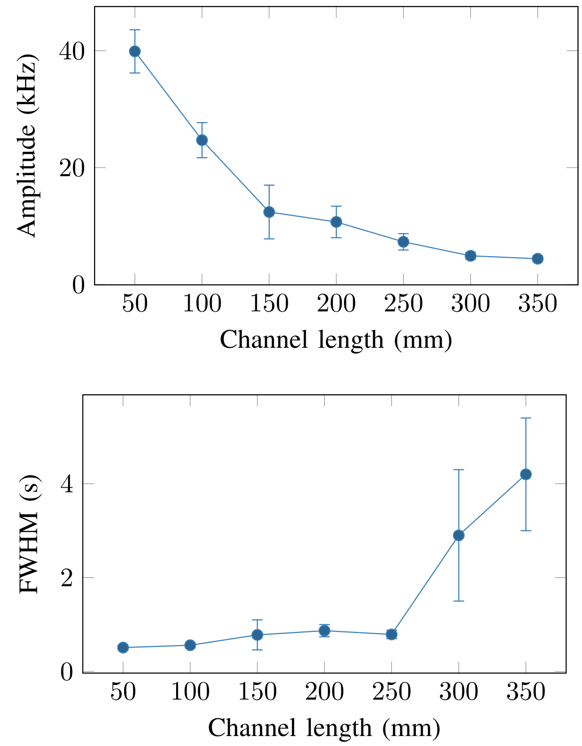

Fig. 5: Maximal resonance shift and FWHM recorded for different channel lengths. The amplitude decreases significantly with an increased channel length while the FWHM rises. The accuracy of FWHM measurement is impacted for long channel lengths by the low signal amplitude.

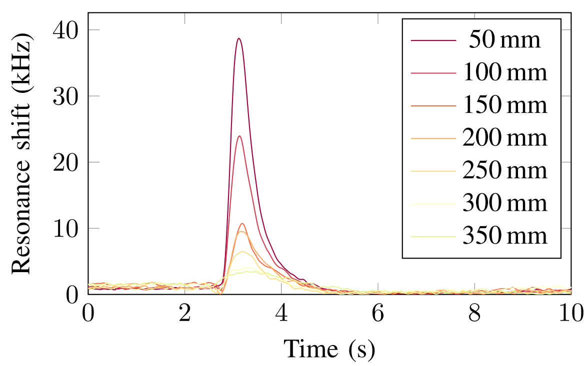

Fig. 6: Impulse responses for varying transmission channel lengths (i.e. distances between the point of injection and the sensor coil).

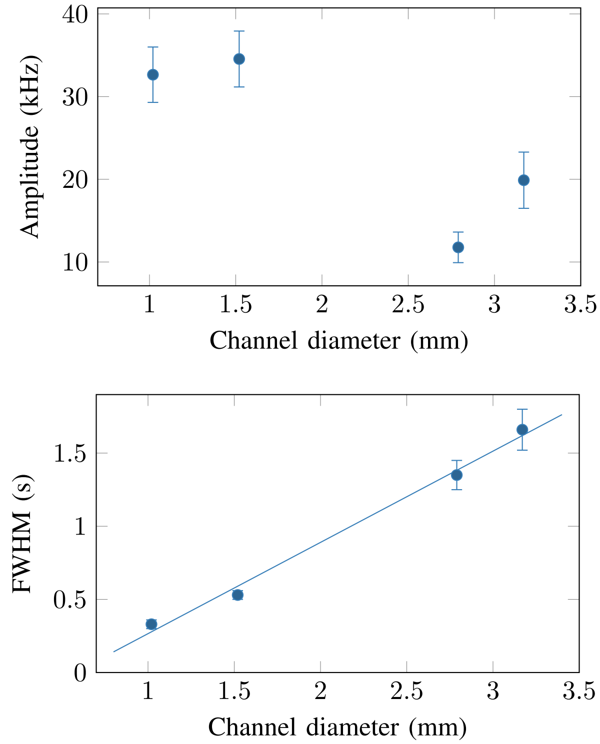

Fig. 7: Variation of the tube diameter used as a transmission channel.

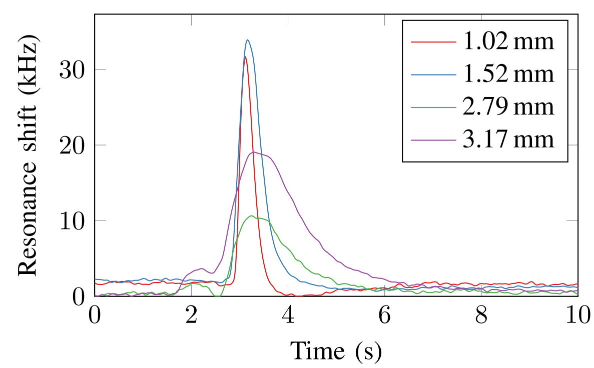

Fig. 8: Impulse responses for four different transmission channels with the specified inner diameter.

in the bent section, acting like a capacitor in an electrical circuit. An initial high concentration of SPIONs is reduced as particles are held in the bend and are washed out over time, contributing to the impulse responses trailing edge. A distinct change in signal shape can be observed in the averaged impulse responses (see Fig. 10).

G. Constricted Channel

Another possible channel variation in a real-life application may be a localised channel constriction, producing a short section with an increased flow velocity. In our setup, a constriction was systematically produced in the middle between the transmitter and receiver using a calliper to squash the flexible transmission tube (with an inner diameter of 1.52 mm and an outer diameter of 3.22 mm) from the outside. The outer diameter was reduced in steps of 0.2 mm to 1.8 mm. The overall thickness of the (flexible) tube wall is 1.7 mm.

As can be seen in Fig. 11, the channel constriction has no prominent effect on the response amplitude or FWHM. This can also be confirmed when comparing the averaged impulse responses in Fig. 12 directly.

The laminar flow criterion $Re < 2300$ in this setup holds for channel diameters larger than 0.09 mm. Therefore, laminar flow is still present for the thinnest constriction (0.1 mm). This explains the consistency of the impulse response for various

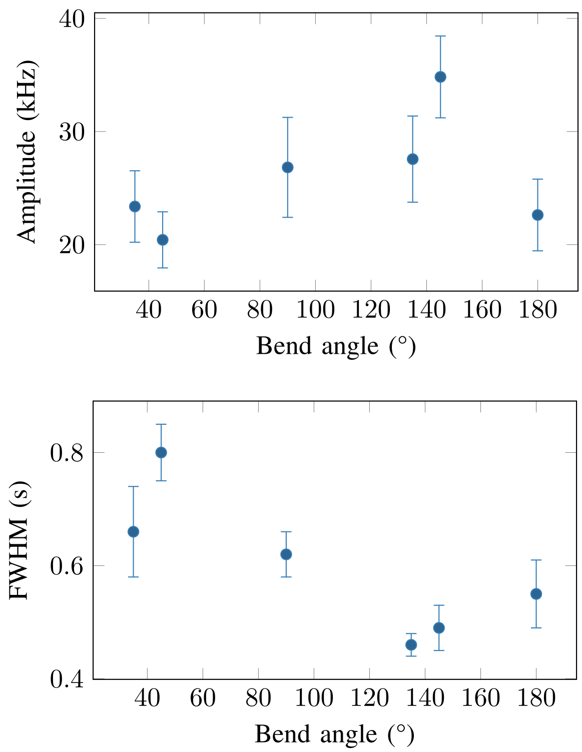

Fig. 9: Amplitude and FWHM for a channel of 100 mm length, bent at a various angles in the middle. Although no overall trend is apparent, an increased FWHM for sharp angles can be observed.

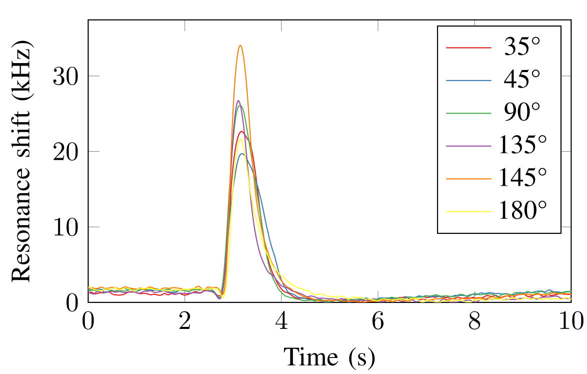

Fig. 10: Impulse responses for a transmission channel with 15 cm length, bent in the middle at the specified angle.

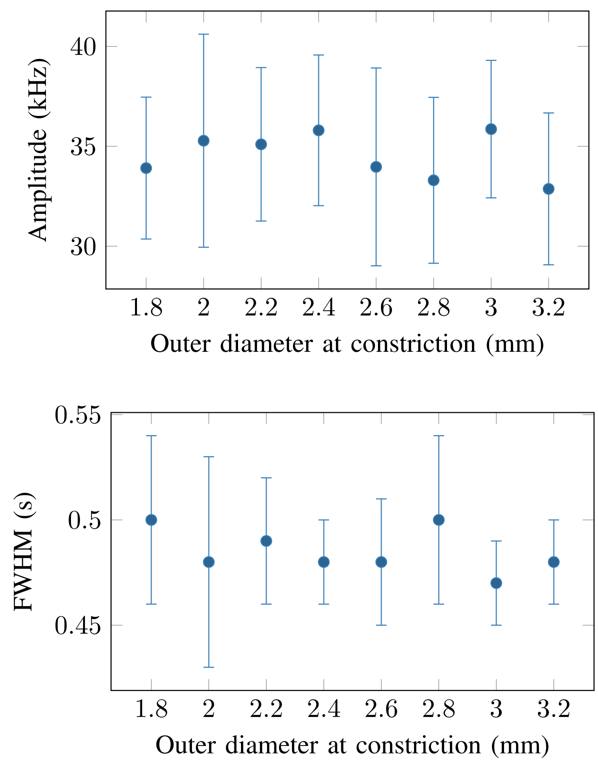

Fig. 11: Amplitude and FWHM for a transmission channel with a localised constriction. The constriction was produced by squashing the tube with a calliper.

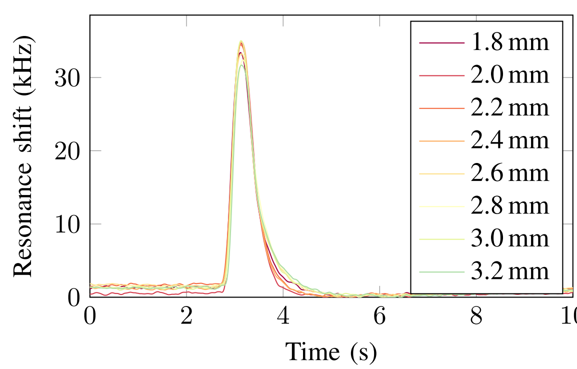

Fig. 12: Averaged impulse responses for a transmission channel with a localised constriction. The legend shows the remaining outer diameter at the constriction. No significant change to the impulse response can be observed.

constriction diameters. In contrast to a systematic change of the channel diameter, a localised section with a changed flow velocity has little effect on the observed impulse response at the receiver.

IV. Transmission Sample

Data transmission can be achieved using the testbed by modulating the injection of SPIONs. Possible transmission schemes include on-off keying [26], [27], concentration shift keying [28], [35], and pulse-position modulation. In [35] a successful data transmission with an effective data rate of 5.5 bit/s was shown.

The data transmission samples were generated using the default testbed parameters (10 mL/min background flow rate, 50 mm long transmission channel, 1.52 mm tube diameter) and the micropump to achieve the modulated injections. The micropump was operated at 250 V and 70 Hz and the injection cannula was fitted with an additional one-way check valve (Darwin Microfluidics) to reduce unwanted back-flow during transmission pauses (see [25] for further details). The various testbed parameters and essential components used for the data transmission samples are listed in Tab. II.

A series of 1000 random symbols was transmitted using on-off keying with symbol interval lengths of 0.75 s and 1 s.

TABLE II: Testbed components and parameters used for the data transmission samples.

Category	Parameter	Value
Transmitter	Micropump	Bartels mp6-liq
	Voltage	250 V
	Frequency	70 Hz
	Injection duration	100 ms
	Injection type	venous cannula with valve
	Injection diameter	0.7 mm
	SPION concentration	7.5 mg/mL
Channel	Tubing material	Tygon LMT-55
	Diameter	1.52 mm
	Length	50 mm
	Background flow pump	Ismatec Reglo ICC
	Background flow rate	10 mL/min
Receiver	Sensor	Texas Instruments LDC1614
	Coil	LDCCOILEVM, Coil K
	Parallel capacitor	68 pF

Each transmission was additionally padded by the sequence

$$00000\,111\,00000\,1\,00000\,10 \tag{4}$$

to simplify automated transmission detection and synchronisation. Each '1' was represented by an activation of the injection pump for 100 ms, whereas no injection was performed for a '0'.

Fig. 13 shows a short transmission sample of the sequence

$$0110111010 \tag{5}$$

for each of the different symbol interval lengths. Due to the long transmission period (up to 17 min), environmental noise throughout a transmission may vary significantly and often causes a drift of the baseline reference.

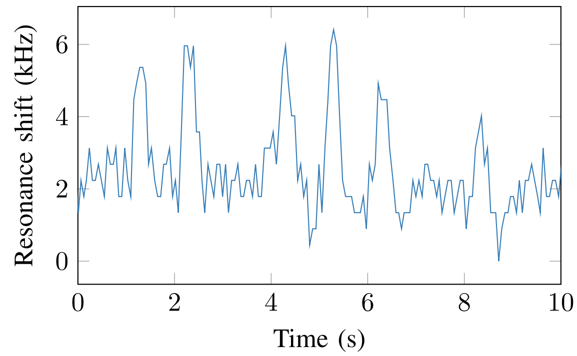

(a) 1.00 s

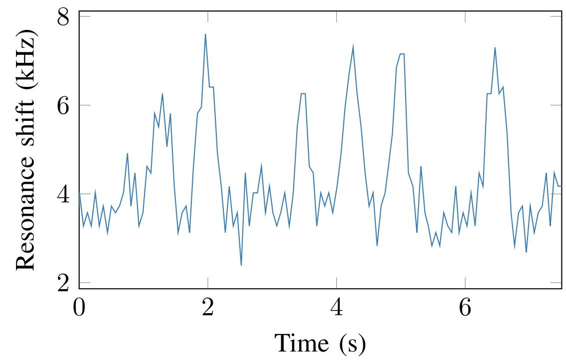

(b) 0.75 s

Fig. 13: Section with ten binary symbols of a large data transmission sample. Each '1' was represented by an injection of SPIONs, visible as a peak in the received signal. Two different symbol interval lengths (1 s and 0.75 s) were used.

V. Data

The raw data for the various channel parameter experiments is provided with this publication (see [36]). The files containing the recorded sensor values for the impulse responses can be found in the folders corresponding to the experiment subsection titles. The data is provided as comma-separated values (csv) files with two columns, one (time) containing the absolute timestamp of the sample in seconds since the beginning of the measurement, and a second column (value) with the resonance frequency measured by the inductance sensor in Hertz.

The recorded sensor data for the transmission samples is also provided in the same format. Additionally, the used random data sequence and the transmitted sequence including the leading and trailing padding are provided as text and csv files.

VI. Summary and Outlook

Various transmission channel parameters, that are potentially relevant in a communication scenario, were investigated in the context of a biocompatible testbed. Often the applicable flow regime (i.e. laminar flow) dominates the impulse response, as could be observed for the channel flow rate or length. An additional minor influence on the FWHM of a changed injection dynamic, caused by an increased background flow rate, was shown.

A localised high flow section, caused by a constriction, has little to no impact on the systems impulse response and is negligible in a transmission scenario. However, a sharp bend acts like an electrical capacitor, leading to a reduced maximal amplitude and an increased FWHM.

A change in channel diameter results in significant changes of both the amplitude and FWHM. Although the variation of the FWHM can somewhat be explained by a changed channel velocity, further investigation into the multiple influence factors, especially the impact of gravity on the used SPIONs, is necessary.

An additional supplement of large data samples, as well as the raw data used for the individual parameter studies, is provided alongside this paper. This enables other researchers to use and work with experimental data for biocompatible molecular communication (e. g. to evaluate channel models, validate simulation results or develop communication protocols), without having to construct their own testbed.

Acknowledgments

This work was supported in part by the German Federal Ministry of Education and Research (BMBF), project MAMOKO (16KIS0913K).

REFERENCES

[1] N. Farsad, H. B. Yilmaz, A. Eckford, C.-B. Chae, and W. Guo, "A comprehensive survey of recent advancements in molecular communication," *IEEE Communications Surveys & Tutorials*, vol. 18, no. 3, pp. 1887–1919, 2016.

[2] N. Farsad, W. Guo, and A. W. Eckford, "Tabletop molecular communication: Text messages through chemical signals," *PLOS ONE*, vol. 8, no. 12, pp. 1–13, Dec. 2013.

[3] M. Damrath, S. Bhattacharjee, and P. A. Hoeher, "Investigation of multiple fluorescent dyes in macroscopic air-based molecular communication," *IEEE Transactions on Molecular, Biological and Multi-Scale Communications*, vol. 7, no. 2, pp. 78–82, 2021.

[4] H. Unterweger, J. Kirchner, W. Wicke, A. Ahmadzadeh, D. Ahmed, V. Jamali, C. Alexiou, G. Fischer, and R. Schober, "Experimental molecular communication testbed based on magnetic nanoparticles in duct flow," in *2018 IEEE 19th International Workshop on Signal Processing Advances in Wireless Communications (SPAWC)*, Jun. 2018, pp. 1–5.

[5] N. Farsad, D. Pan, and A. Goldsmith, "A novel experimental platform for in-vessel multi-chemical molecular communications," in *GLOBECOM 2017 - 2017 IEEE Global Communications Conference*. IEEE, Dec. 2017, pp. 1–6.

[6] L. Grebenstein, J. Kirchner, R. S. Peixoto, W. Zimmermann, F. Irnstorfer, W. Wicke, A. Ahmadzadeh, V. Jamali, G. Fischer, R. Weigel, A. Burkovski, and R. Schober, "Biological optical-to-chemical signal conversion interface: A small-scale modulator for molecular communications," *IEEE Transactions on NanoBioscience*, vol. 18, no. 1, pp. 31–42, Jan. 2019.

[7] T. Nakano, T. Suda, M. Moore, R. Egashira, A. Enomoto, and K. Arima, "Molecular communication for nanomachines using intercellular calcium signaling," in *2005 5th IEEE Conference on Nanotechnology*. Piscataway, N.J: IEEE Service Center, 2005, pp. 632–635.

[8] P. Lu, Z. Wu, and B. Liu, "A vertical channel model of molecular communication and its test-bed," *EAI Endorsed Transactions on Pervasive Health and Technology*, vol. 3, no. 9, 3 2017.

[9] N.-R. Kim, N. Farsad, C.-B. Chae, and A. W. Eckford, "A realistic channel model for molecular communication with imperfect receivers," in *2014 IEEE International Conference on Communications (ICC)*, 2014, pp. 3987–3992.

[10] N.-R. Kim, N. Farsad, C. Lee, A. W. Eckford, and C.-B. Chae, "An experimentally validated channel model for molecular communication systems," *IEEE Access*, vol. 7, pp. 81 849–81 858, 2019.

[11] P. N. Prasanth, K. P. Sumanth, V. K. Chakka, and G. Roy, "Experimental implementation of molecular communication system using sampling based adaptive threshold variation demodulation algorithm," in *2018 IEEE International Conference on Advanced Networks and Telecommunications Systems (ANTS)*, 2018, pp. 1–5.

[12] A. O. Kislal, B. C. Akdeniz, C. Lee, A. E. Pusane, T. Tugcu, and C.-B. Chae, "Isi-mitigating channel codes for molecular communication via diffusion," *IEEE Access*, vol. 8, pp. 24 588–24 599, 2020.

[13] F. Gulec and B. Atakan, "A droplet-based signal reconstruction approach to channel modeling in molecular communication," *IEEE Transactions on Molecular, Biological and Multi-Scale Communications*, vol. 7, no. 1, pp. 64–68, 2021.

[14] B.-H. Koo, C. Lee, H. B. Yilmaz, N. Farsad, A. Eckford, and C.-B. Chae, "Molecular MIMO: From theory to prototype," *IEEE Journal on Selected Areas in Communications*, vol. 34, no. 3, pp. 600–614, Mar. 2016.

[15] D. T. McGuiness, S. Giannoukos, S. Taylor, and A. Marshall, "Experimental and analytical analysis of macro-scale molecular communications within closed boundaries," *IEEE Transactions on Molecular, Biological and Multi-Scale Communications*, vol. 5, no. 1, pp. 44–55, 2019.

[16] S. Giannoukos, A. Marshall, S. Taylor, and J. Smith, "Molecular communication over gas stream channels using portable mass spectrometry," *J. Am. Soc. Mass Spectrom*, vol. 28, pp. 2371–2383, 2017.

[17] B.-H. Koo, H. J. Kim, J.-Y. Kwon, and C.-B. Chae, "Deep learning-based human implantable nano molecular communications," in *ICC 2020 - 2020 IEEE International Conference on Communications (ICC)*, 2020, pp. 1–7.

[18] A. Al-Helali, B. Liang, and N. Nasser, "Novel molecular signaling method and system for molecular communication in human body," *IEEE Access*, vol. 8, pp. 119 361–119 375, 2020.

[19] L. Wang, N. Farsad, W. Guo, S. Magierowski, and A. W. Eckford, "Molecular barcodes: Information transmission via persistent chemical tags," in *2015 IEEE International Conference on Communications (ICC)*. IEEE, Jun. 2015, pp. 1097–1102.

[20] L. Grebenstein, J. Kirchner, W. Wicke, A. Ahmadzadeh, V. Jamali, G. Fischer, R. Weigel, A. Burkovski, and R. Schober, "A molecular communication testbed based on proton pumping bacteria: Methods and data," *IEEE Transactions on Molecular, Biological and Multi-Scale Communications*, vol. 5, no. 1, pp. 56–62, 2019.

[21] L. Khaloopour, S. V. Rouzegar, A. Azizi, A. Hosseinian, M. Farahnak-Ghazani, N. Bagheri, M. Mirmohseni, H. Arjmandi, R. Mosayebi, and M. Nasiri-Kenari, "An experimental platform for macro-scale fluidic medium molecular communication," *IEEE Transactions on Molecular, Biological and Multi-Scale Communications*, vol. 5, no. 3, pp. 163–175, 2019.

[22] T. Luo, R. Zheng, J. Song, L. Lin, and H. Yan, "A small-scale modulator of electric-to-biological signal conversion for synthetic molecular communications," in *ICC 2020 - 2020 IEEE International Conference on Communications (ICC)*, 2020, pp. 1–7.

[23] C. Janko, J. Zaloga, M. Pöttler, S. Dürr, D. Eberbeck, R. Tietze, S. Lyer, and C. Alexiou, "Strategies to optimize the biocompatibility of iron oxide nanoparticles – "spions safe by design"," *Journal of Magnetism and Magnetic Materials*, vol. 431, pp. 281–284, 2017.

[24] T. Neuberger, B. Schöpf, H. Hofmann, M. Hofmann, and B. von Rechenberg, "Superparamagnetic nanoparticles for biomedical applications: Possibilities and limitations of a new drug delivery system," *Journal of Magnetism and Magnetic Materials*, vol. 293, no. 1, pp. 483–496, 2005, proceedings of the Fifth International Conference on Scientific and Clinical Apllications of Magnetic Carriers.

[25] M. Bartunik, G. Fischer, and J. Kirchner, "The development of a biocompatible testbed for molecular communication with magnetic nanoparticles," *IEEE Transactions on Molecular, Biological and Multi-Scale Communications*, 2023.

[26] M. Bartunik, M. Lübke, H. Unterweger, C. Alexiou, S. Meyer, D. Ahmed, G. Fischer, W. Wicke, V. Jamali, R. Schober, and J. Kirchner, "Novel receiver for superparamagnetic iron oxide nanoparticles in a molecular communication setting," in *Proceedings of the Sixth Annual ACM International Conference on Nanoscale Computing and Communication - NANOCOM '19*. ACM Press, Sep. 2019, pp. 1–6.

[27] M. Bartunik, H. Unterweger, C. Alexiou, R. Schober, M. Lübke, G. Fischer, and J. Kirchner, "Comparative evaluation of a new sensor for superparamagnetic iron oxide nanoparticles in a molecular communication setting," in *Bio-inspired Information and Communication Technologies*. Cham: Springer International Publishing, 2020, pp. 303–316.

[28] M. Bartunik, T. Thalhofer, C. Wald, M. Richter, G. Fischer, and J. Kirchner, "Amplitude modulation in a molecular communication testbed with superparamagnetic iron oxide nanoparticles and a micropump," in *Body Area Networks. Smart IoT and Big Data for Intelligent Health*, M. M. Alam, M. Hämäläinen, L. Mucchi, I. K. Niazi, and Y. Le Moullec, Eds. Cham: Springer International Publishing, 2020, pp. 92–105.

[29] M. Bartunik, J. Reichstein, and J. Kirchner, "Capacitive sensing for magnetic nanoparticles in molecular communication," in *2022 IEEE International Instrumentation and Measurement Technology Conference (I2MTC)*, 2022, pp. 1–5.

[30] M. Bartunik, S. Faghih-Naini, T. Maiwald, and J. Kirchner, "Planar coils for detection of magnetic nanoparticles in a testbed for molecular communication," in *Proceedings of the 9th ACM International Conference on Nanoscale Computing and Communication*, J. M. Jornet and M. Pierobon, Eds. New York, NY, USA: ACM, 2022, pp. 1–6.

[31] R. Tietze, S. Lyer, S. Dürr, T. Struffert, T. Engelhorn, M. Schwarz, E. Eckert, T. Göen, S. Vasylyev, W. Peukert, F. Wiekhorst, L. Trahms, A. Dörfler, and C. Alexiou, "Efficient drug-delivery using magnetic nanoparticles–biodistribution and therapeutic effects in tumour bearing rabbits," *Nanomedicine : nanotechnology, biology, and medicine*, vol. 9, no. 7, pp. 961–971, 2013.

[32] F. M. White, *Fluid mechanics*, 8th ed. New York: McGraw-Hill Education, 2017.

[33] H.-L. Liang, "Doppler flow measurement of lower extremity arteries adjusted by pulsatility index," *American Journal of Roentgenology*, vol. 214, no. 1, pp. 10–17, 2020, pMID: 31670583.

[34] W. F. Blair, R. J. Morecraft, T. D. Brown, and R. H. Gabel, "Transcutaneous blood flow measurements in arteries of the human hand," *The Journal of Hand Surgery*, vol. 16, no. 1, pp. 169–175, 1991.

[35] M. Bartunik, O. Keszocze, B. Schiller, and J. Kirchner, "Using deep learning to demodulate transmissions in molecular communication," in *2022 IEEE 16th International Symposium on Medical Information and Communication Technology (ISMICT)*. IEEE, 2022, pp. 1–6.

[36] M. Bartunik, "Channel parameter studies with a biocompatible testbed for molecular communication," IEEE Dataport, 2023.

Max Bartunik (Graduate Student Member, IEEE) completed his master's degree for electrical engineering in 2019 at the Friedrich-Alexander-Universität Erlangen-Nürnberg (FAU). He is currently pursuing his Ph.D. as a research assistant at the Institute for Electronics Engineering of the FAU. His main research topics are molecular communication and medical electronics.

Janina Teller studied industrial engineering at FAU and completed her bachelor's degree in 2020 with a thesis in the field of molecular communication. She is currently finishing her master's degree and is working on filter design for power electronics.

Georg Fischer (Senior Member, IEEE) received the Diploma degree in electrical engineering with a focus on communications and microwave from RWTH Aachen University, Aachen, Germany, in 1992, and the Dr. Ing. degree in electrical engineering from the University of Paderborn, Germany, in 1997. From 1993 to 1996, he was a Research Assistant with the University of Paderborn, where he was involved in adaptive antenna array systems for mobile satellite communications. From 1996 to 2008, he performed research with Bell Laboratories, Lucent (later Alcatel-Lucent), where he focused on the RF and digital architecture of mobile communication base stations for global system for mobile communications (GSM), universal mobile telecommunications system, and features for network coverage and capacity enhancements. In 2000, he became a Bell Laboratories Distinguished Member of Technical Staff, and in 2001, he became a Bell Laboratories Consulting Member of Technical Staff. He also acted as the Chairman of the European Telecommunications Standards Institute during the physical-layer standardization of the GSM-EDGE system. From 2001 to 2007, he was a part-time Lecturer with the University of Erlangen-Nuremberg, Germany. During that time, he lectured on base station technology. Since 2008, he is a Professor of Electronics Engineering with the University of Erlangen–Nuremberg. He holds over 50 patents concerning microwave and communications technology. His current research interests concentrate on medical electronics, such as using microwaves for detection of vital parameters. He is also a Senior Member of the IEEE Microwave Theory and Techniques, Antennas and Propagation, Computer Society, and Vehicular Technology Society and a member of VDE-ITG and the European Microwave Association.

Jens Kirchner (Senior Member, IEEE) studied physics at FAU and at University of St. Andrews, Scotland. He received his doctorates in 2008 and 2016 from FAU in the fields of biosignal analysis and philosophy of science to the Dr. rer. nat. and Dr. phil, respectively. Between 2008 and 2015 he worked at Biotronik SE & Co. KG in Erlangen and Berlin in the research and development of implantable cardiac sensors. Since 2015, he is with the Institute for Electronics Engineering at FAU, where he heads the Medical Electronics & Multiphysics Systems group. His research interests lie in wearable and implantable sensors, inductive power transfer, and molecular communication. He is a Senior Member of the IEEE with membership in the Communications Society, the Magnetics Society and the Engineering in Medicine and Biology Society.